

Kinetics of layer-thinning transitions in overheated smectic films

S. Pankratz, P. M. Johnson, A. Paulson, and C. C. Huang

School of Physics and Astronomy, University of Minnesota, Minneapolis, Minnesota 55455

(Received 23 November 1999)

The kinetic behavior of dislocation loops in overheated free-standing smectic-A films is reported. The loops open at velocities that are much faster than those seen in nonoverheated films. The velocities increase dramatically as a function of temperature and vary slightly as a function of film thickness. The behavior of dislocation loops induced with a pulsed resistive wire heater is identical to that of the loops giving rise to the layer-thinning transition. In addition, the interaction between two simultaneously nucleated dislocation loops is analyzed. The observed interactions give evidence that thinning occurs in the interior of the film. The results support a model for the layer-by-layer thinning transition based on the nucleation of dislocation loops.

PACS number(s): 64.70.Md, 61.30.-v

I. INTRODUCTION

Liquid crystals have long been used successfully to study a variety of phenomena, including defects and surface interactions in an ordered fluid [1–3]. Particularly useful in these studies is the fact that many smectic liquid crystals can be made to span an opening as a free-standing film. This geometry allows for the study of monodomain, substrate-free, variable thickness liquid-crystal films. In most liquid crystals, the degree of smectic order is strengthened by the presence of a free surface. This increased order can cause a layered structure to exist at the surface of a bulk sample above the temperature range of its bulk smectic phase. Surface-enhanced ordering can stabilize some liquid-crystal free-standing films well into the bulk isotropic temperature range. Of these compounds, a handful undergo layer-by-layer thinning as the temperature is increased. In this process, an overheated smectic film decreases in multiple- and single-layer steps as the temperature is increased [4]. We have found that all compounds that display regular and reproducible layer-by-layer thinning share the common feature of being fluorinated in one or both tails [4–7]. Irregular thinning transitions have been reported in several conventional and nonfluorinated compounds [8–11]. In this paper, we present optical measurements and video observations that reveal the nature and kinetics of the layer-thinning transition.

Unlike the free-standing films of most liquid-crystal compounds, a typical thick (>20 layers) film of a fluorinated compound that exhibits the layer-thinning transition does not rupture when heated above the bulk smectic-A–isotropic transition temperature (T_{AI}). In contrast, it undergoes a series of thinning transitions in which the film thickness decreases in a stepwise manner. For example, the thickness, in smectic layers (N), might exhibit the following thinning series: $N=15, 11, 9, 8, 7, 6, 5, 4, 3$, and 2 as the film temperature is increased. The two-layer film ruptures at a temperature approximately 30 K above T_{AI} . The thinning transition is thermally driven and irreversible. For example, a two-layer film does not rupture for more than 5 h at 20 K above T_{AI} and does not spontaneously thicken when cooled well into the smectic-A (Sm-A) phase [12]. Moreover, a film of N layers or less can be spread and will remain stable at temperatures below the thinning temperature [$T_C(N)$] for the

N -layer film even though the film temperature is above T_{AI} . The thinning temperatures of independently prepared films are reproducible to within a fraction (a few hundred mK) of 1° . The temperature of the final rupture of the two-layer film may vary up to 2° or 3° . Recently, in a compound with two fluorinated tails, single-layer thinning was observed from 25 down to two layers [7].

The layer-thinning transition has been modeled as the successive melting and subsequent removal of interior layers of the film as the global film temperature is increased in the range $T > T_{AI}$ or $T > T_{AN}$ [13–15]. Here T_{AN} denotes the bulk Sm-A–nematic transition temperature. The enhanced smectic order at the free surface of the film penetrates into the film a distance on the order of ξ , the smectic correlation length. As this quantity decays with increasing temperature, the film thickness for which the interior layer can be stabilized decreases. In these models, when ξ for an N -layer film is reduced to less than half the film thickness, the interior layer becomes disordered and melts, causing the layer to collapse and the material to be moved from the film into the surrounding bulk reservoir. Thus the thinning occurs only after the interior layer has melted into the nematic or isotropic phase. According to the results of our optical reflectivity measurements described below, this scenario is unlikely, at least on a macroscopic scale.

Recently, a different model was proposed, based on the one presented by Géminard *et al.* [16], in which the condition necessary for a thinning to occur is not the melting of the interior layer, but the formation of a dislocation loop [17]. As the smectic order of the interior layer of the film decreases with increasing temperature, the energy cost for nucleating a dislocation loop large enough not to collapse under its own line tension decreases. When the nucleation energy becomes comparable to the thermal energy $k_B T$, a growing loop is nucleated at a random location. This model also predicts a sharp, steplike boundary between the expanding thin region and the rest of the film, since the dislocation loop exists in a defined layer structure. In addition, the presence of line tension favors a circular loop when the radius is small. To gain further insight into the thinning phenomenon, we have studied the kinetics and time evolution of many layer thinnings. The compound used in this study is H8F(4, 2, 1)MOPP, in which the hydrogen atoms in one of the flex-

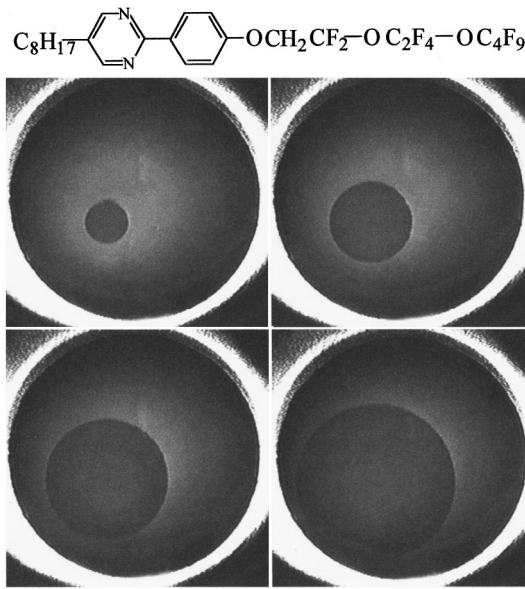


FIG. 1. Photographs showing a growing, single-layer dislocation loop that spontaneously nucleated in a four-layer film as the temperature was raised above $T_c(4)$. Note the circular shape and sharp loop boundary. The time between pictures is 150 ms.

ible tails are mostly replaced by fluorine atoms (see Fig. 1).

II. EXPERIMENTAL RESULTS AND DISCUSSIONS

One of the dynamical quantities characterizing the layer-thinning process is the velocity of the thinning front. We have designed a system to directly measure this velocity. A collimated white light beam is used to illuminate the entire film and the reflected image of the film is recorded using a charge-coupled-device camera and video cassette recorder. Thickness changes of single smectic layers (~ 30 Å) are clearly visible in thin films (2–15 layers). Using this method, the origin of a thinning and the evolving shape and relative sharpness of its boundary can be determined. The film thickness is also monitored using a 633-nm He-Ne laserbeam focused to a spot (~ 0.5 mm diam) to measure the optical reflectivity of the film [5]. The reflectivity is a sensitive measure of film thickness to within a resolution of 1 Å [12]. The size of our free-standing films is about 3 cm². The optical reflectivity remains constant until the thinning front passes through it, indicating that the layer structure surrounding the dislocation loop is unchanged. Figure 1 shows four video frames of a four- to three-layer thinning that occurred spontaneously as the temperature was increased. The velocity of a thinning front is obtained by measuring the distance from the origin of a thinning to its expanding edge for successive video frames. The distance increases linearly with time, as shown in Fig. 2. The slope gives the velocity (~ 1.7 cm/s).

A. Single thinning loops

In order to determine the thickness and temperature dependence of the thinning velocity, it is necessary to obtain thinning velocity data both for different film thicknesses at the same temperature and for a single film thickness at different temperatures. This requires thinnings to occur in films

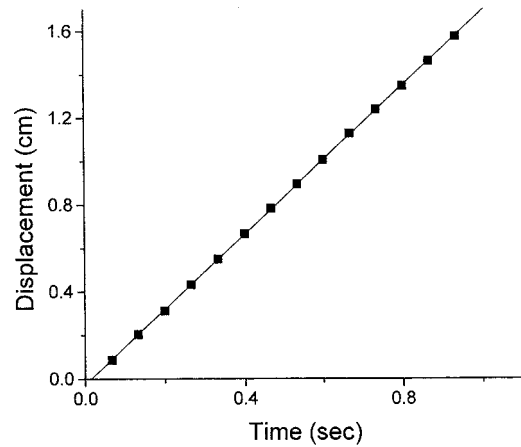


FIG. 2. Displacement of the thinning front from the nucleation origin for a 4→3 layer thinning. The slope of the linear fit yields the thinning speed.

that are not near the thermodynamic condition for spontaneous thinning. Thus the process must be initiated by a localized external source such that the thermodynamic state of the film away from the thinning origin is unaffected. To achieve this we use an approach recently developed by Géminard *et al.* [16]. A 2-mm-long piece of constantan wire, 75 μm diam, folded to a point, is used as a localized heat source. This heater is positioned within 100 μm of the film. By raising the temperature briefly and locally using a short (~ 1 ms), precisely controlled voltage pulse applied to the wire heater, we can initiate thinning transitions at the heater tip while the rest of the film remains at temperatures $T < T_c(N)$ [18]. Here $T_c(N)$ is the spontaneous thinning transition temperature for an N -layer film to an $(N-1)$ -layer film. When the temperature of an N -layer film is near $T_c(N)$, only a small voltage pulse $V_N(T)$ is necessary to produce a one-layer thinning. If a larger pulse is applied, two- and three-layer thinning transitions can be initiated. These multilayer thinnings are further discussed below. As $\Delta T_N = T_c(N) - T$ increases, the required thinning voltage $V_N(T)$ increases. If ΔT_N becomes too large, a single-layer thinning can no longer be induced and an increase in the applied voltage pulse instead causes a multilayer thinning or ruptures the film.

Velocity data from induced dislocation loops at different film thicknesses and temperatures are compiled in Fig. 3. The dislocation loop induced by a thermal pulse expands at a

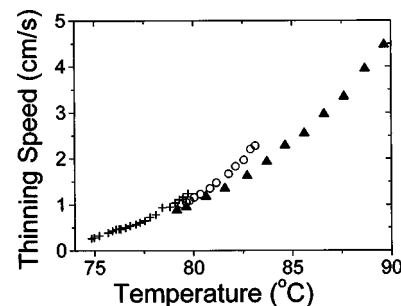


FIG. 3. Thinning speed of single-layer thinnings in five-layer films (crosses), four-layer films (open circles), and three-layer films (triangles) as a function of temperature.

constant rate, just as for the spontaneous thinning shown in Figs. 1 and 2. The temperature range of each film thickness shown is limited at the high end by the spontaneous thinning temperature $T_C(N)$, and at the low end by our inability to initiate a single-layer thinning. The velocities of these fronts, even just above T_{AI} , are three to four orders of magnitude greater than those measured by Géminard *et al.* [16] in the bulk Sm-A phase window. As we shall discuss below, this comes as a result of a force of physically different origin driving the expansion of the fronts. Single-layer, expanding dislocation loops could not be thermally nucleated below T_{AI} . The mechanism in [16] relied on a nearly second-order Sm-A–nematic (N) transition. An applied heat pulse could bring a local region of the film arbitrarily close to this transition temperature (T_{AN}), and the Sm-A order then decreased locally to the point at which the layer collapsed, forming a dislocation loop. In our case, the Sm-A–isotropic transition is first order, so the smectic order does not smoothly decrease to zero at the transition. The fluorinated compounds also have a very high degree of smectic order even as T_{AI} is approached. We found that upon applying a heat pulse, nothing occurred until the heat pulse was large enough to melt material locally and form thicker multilayer loops or droplets that would invariably collapse. We can, however, deduce an order of magnitude speed for single-layer dislocation loops below T_{AI} , because these are often seen in an initially non-uniform film immediately after spreading. The rate of these is comparable to values found for the ordinary liquid crystals (on the order of $\mu\text{m}/\text{sec}$), rather than cm/sec as seen in our system above T_{AI} .

It is immediately clear from Fig. 3 that the temperature is the most important factor in determining the thinning velocity. For a given film thickness, the velocity increases as T is raised. Note also that near 79°C , it is possible to thin the film from five to two layers in single-layer steps at a single temperature. For a given temperature, the velocity of the thinning front becomes larger with increasing thickness. This thickness dependence indicates that it is very unlikely that the thinning front is located in one of the outermost layers. As will be explained below, this result is consistent with the model in which a thinning is the result of a nucleated dislocation loop within the weak interior Sm-A layer [17,19].

We explain these results qualitatively using a recent model by Pankratz *et al.* [17]. In this model, a pressure difference Δp exists between the film and the surrounding bulk reservoir to maintain thermodynamic equilibrium, $\Delta G = -f_{I \rightarrow A}(T) + \Delta p = 0$. Here the first term is due to the entropy difference between the overheated Sm-A film and the isotropic bulk reservoir. It should depend on the degree of overheating. Δp represents the work necessary to move material from the film to the bulk reservoir against the pressure difference. Thus Δp should be the same for all films at a given temperature. Once a dislocation loop has been formed, Δp provides the driving force for its growth. The line tension and layer sliding viscosity oppose the expansion of the loop. For loop sizes greater than a few hundred micrometers, the force on the loop due to the line tension becomes insignificant compared to the driving force, and the shear viscosity between the layer being removed and its neighboring layers becomes the significant retarding force. During a single-layer thinning, the shear viscosity should be related to the degree

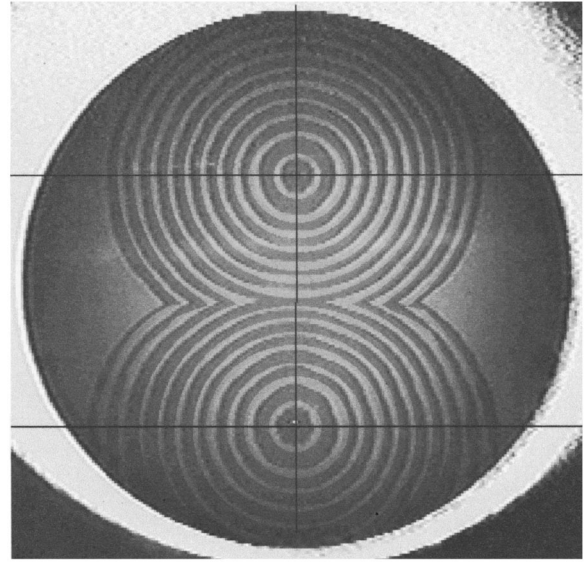


FIG. 4. Compilation of 11 video frames of a one-layer thinning in a five-layer film. The four-layer dark regions merge when the two thinning fronts meet.

of smectic ordering. Based on a theory by de Gennes [20] for the presmectic ordering between two walls, the magnitude of the smectic order at the center of an N -layer film for $T > T_{AI}$ has the following form:

$$|\Psi|^2 = h_x^2 \xi^2 / \sin^2(Nd/2\xi), \quad (1)$$

where $\xi = \xi_o(T/T_C - 1)^{-1/2}$ [17]. For a given temperature, the smectic order at the film center increases with decreasing thickness. Thus a growing dislocation loop in the center layer of an N -layer film experiences the same driving force (Δp) as one in an $(N-1)$ -layer film at the same temperature, but the magnitude of its shear viscosity is smaller due to the lesser degree of smectic ordering. This argument explains the observed increase of the thinning velocity with film thickness. According to Eq. (1), the smectic order, and hence the viscous force, decreases with increasing temperature. In addition, according to the condition for thermodynamic equilibrium [17], Δp (and hence the driving force) should increase as the film is further overheated. Both the decreasing viscosity and the increasing driving force give rise to the observed increase in thinning velocity as the temperature is increased. Currently, we are still looking for a suitable theoretical model with which to describe our experimental findings.

B. Interactions between two thinnings

In addition to single dislocation loops, we have studied the interaction between two loops nucleated simultaneously at a distance 1 cm apart. The loops are induced using two pulse heaters that are both triggered from the same power supply. By adjusting the voltage applied to each heater separately, it is possible to cause thinnings with equal or unequal total Burgers vectors to expand radially and approach each other. Figure 4 is a compilation of 11 video frames of two single-layer thinnings nucleated in a five-layer film. The dark regions are one layer thinner than the light regions. As can

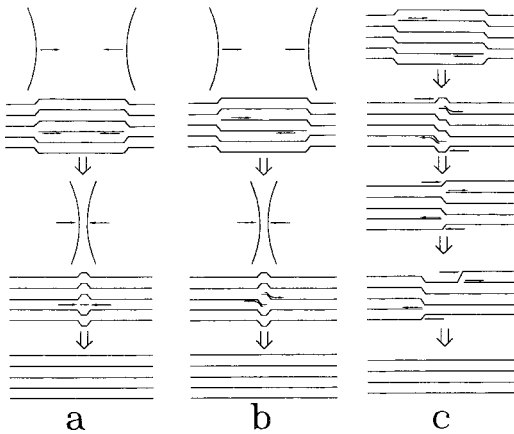


FIG. 5. Possible thinning scenarios for two one-layer thinnings in a six-layer film. (a) Both loops are nucleated in the same interior layer. (b) The two loops exist in adjacent interior layers. (c) The loops are nucleated near opposite surfaces of the film.

be seen, when the two circles meet, the thin regions coalesce into a connected area that is four layers thick, and this behavior is observed in all the single-layer thinnings. As we shall explain below, this finding supports our previous observation that the thinnings occur in the interior of the film and not at the surfaces. The region where the two circles meet remains a very sharp V shape as the thinning region increases. This confirms our assertion that the effect of the line tension is fairly small relative to the viscous and driving forces on the loop edge for a sufficiently large dislocation loop.

Several thinning scenarios are possible. If the dislocation loops exist and expand in the same interior layer, the two thinner regions will naturally merge upon contact. If they exist in adjacent interior layers, they can also effectively merge, as the two dislocations of opposite Burgers vectors collapse upon meeting. These cases are schematically shown in Figs. 5(a) and 5(b). In contrast, a thinning involving two dislocations in nonadjacent layers separated by one or more smectic layers, which are well defined according to the previously mentioned optical studies, cannot easily collapse when they meet. If each of the two dislocations nucleates at or near a surface rather than in the interior, there should be a finite probability both for their formation near the same surface and for formation near opposite surfaces. If such surface dislocations occurred, we should observe two cases: one in which two single-layer thinnings occurring near the same surface merge, resulting in a film that is one layer thinner, and another in which the dislocation loops (near opposite surfaces) cross and proceed to produce a two-layer thinning. The last scenario is depicted in Fig. 5(c) but in more than 100 single-layer thinning transitions observed during the course of this experiment it has not been observed. We conclude from this argument that the dislocation loops are nucleated at or near the center of the film.

In addition to simultaneously generating two single-layer dislocation loops, we have obtained detailed time evolution of the following pairs of thinning steps: $(4 \rightarrow 3, 4 \rightarrow 2)$, $(5 \rightarrow 4, 5 \rightarrow 3)$, $(4 \rightarrow 2, 4 \rightarrow 2)$, and $(5 \rightarrow 2, 5 \rightarrow 4)$. The time evolution for the last case is shown in Fig. 6. Three separate fronts are clearly visible in the three-layer (3L) thinning. After meeting the single-layer (1L) dislocation loop, the

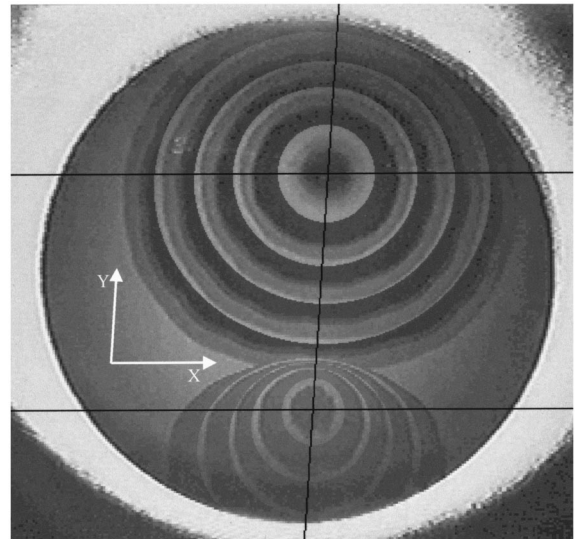


FIG. 6. Compilation of five video frames of a three-layer thinning (top) meeting a one-layer thinning (bottom) in an initially five-layer film. Note the dramatic slowing of the one-layer front upon meeting the three-layer thinning front.

steps of the remaining two-layer thinning keep moving ahead into the four-layer-thick region. The positions of the 1L thinning front when meeting a 2L and a 3L thinning are plotted in Fig. 7 along two perpendicular directions, i.e., x and y as a function of time. Here the y direction is along the line joining the two small heaters. While the velocities of the fronts remain fairly constant in the x direction, those along the y direction behave very differently. In this direction, the front from the single-layer dislocation loop slows down significantly and almost becomes stationary before meeting the first front of the three-layer thinning step. In addition, its speed in the opposite ($-y$) direction appears to be larger than in the horizontal direction. Table I lists the initial and meeting speeds of each pair of thinning steps having various total combined Burgers vectors. In the first four cases, pairs of thinning steps having the same total Burgers vector (one or two) yield about the same meeting speed (as a percentage of initial speed) for each pair. In the last three, the meeting

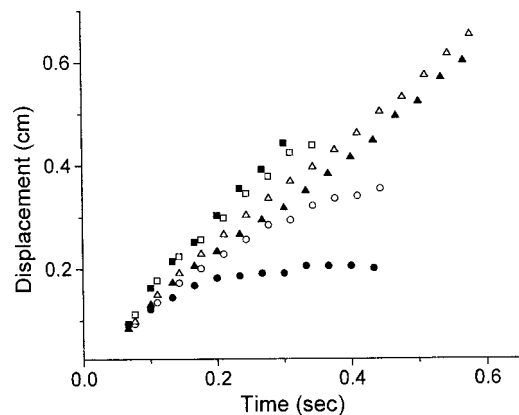


FIG. 7. Displacement of a thinning front from its origin for a $5 \rightarrow 4$ layer thinning meeting a $5 \rightarrow 3$ layer thinning (open) and meeting a $5 \rightarrow 2$ layer thinning (solid). The displacement was measured in the forward direction (circles), the backward direction (squares), and the sideways direction (triangles).

TABLE I. Speeds of thinning fronts just prior to meeting for several pairs of thinning transitions. The disparity in meeting speed is largest for the bottom three pairs, in which the thinning fronts involve unequal numbers of layers.

Thinning	Initial speed (cm/s)	Meeting speed (cm/s)	Meeting speed (% of initial speed)
5-4	0.85	0.50	59
5-4	0.80	0.60	75
4-3	1.0	0.80	80
4-3	1.0	0.70	70
3-2	3.25	1.8	55
3-2	3.35	2.2	65
4-2	1.0	0.50	50
4-2	1.1	0.68	62
4-3	0.88	0.22	25
4-2	1.3	1.0	77
5-4	1.2	0.42	35
5-3	1.65	0.92	56
5-4	0.85	0	0
5-2	1.55	1.4	90

fronts have unequal total Burgers vectors and show larger differences in the meeting speeds.

In order to address these features, we propose a picture of a 3L and 1L thinning in a five-layer film as shown in Fig. 8. Here lines indicate the center of mass of the smectic layers. If the interior layers are being removed, then for the 3L thinning all layers are moving except the outer two. The three layers move with roughly the same speed, as is seen in Fig. 6. Thus for three layers sliding together there are two layer surfaces sliding next to stationary neighbor layers. A single sliding layer also has two such sliding surfaces, resulting in a higher per-layer viscous force. The driving force per unit length per layer is $d\Delta p$, indicating that the driving force on a 3L front is three times the force on a 1L front. This explains why the rate of expansion for a multiple-layer thinning loop is larger than for a single-layer loop. By assuming that the thinnings occur in the center of the film, we can also explain the direction dependence of the velocity of the 1L dislocation. The shear force is determined by the relative velocity between layers as they slide out of the film. Thus we expect the velocity of the 1L loop relative to its neighbors to be roughly independent of direction. As shown in Fig. 7, the one-layer dislocation moves faster as it slides with its neigh-

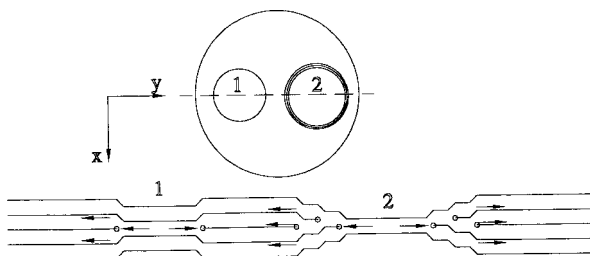


FIG. 8. Top and cross-sectional view of proposed film structure for the thinnings of Fig. 6. Lines indicate the layer center of masses, and arrows the direction of motion.

bors and away from the origin of the 3L. In contrast, the front of the one-layer thinning in the region moving toward the 3L thinning origin must move slower to maintain the same relative velocity with neighbors. Notice that for the 1L dislocation meeting a 2L thinning (Fig. 7), the effect on the speed is noticeable but smaller, as only one of the two neighboring layers is moving. As the radius R of the 3L (2L) thinning front grows at a constant rate, the speed of the material at a given point ahead of it will increase linearly with R , and this will also tend to slow down the opposing 1L front. An additional slowing effect is the fact that two opposite defects are expanding in the same layer, forcing material in the region between the two defects to slide in the $\pm x$ direction to the meniscus (Figs. 6 and 8). If the velocity of the neighboring layers is large enough and in the opposite direction of the 1L thinning, the thinning front may actually stop as is seen experimentally. Note finally that the motion of neighboring layers in a direction perpendicular to the direction of the expanding front should, by the above reasoning, have a minimal effect on the velocity, and this is the observed behavior (Fig. 8). In the above explanations, only a qualitative description is given, as the total viscous force on a segment of loop is due to the force on all the contributing areas of the sliding layer, and the relative velocity of neighboring layers changes continuously between different locations in the film.

C. Other phenomena

The application of a large heat pulse to an overheated free-standing film produced other phenomena that are worth mentioning here. When a large pulse amplitude is used at temperatures less than 2° above T_{A1} the meniscus is seen to briefly (30–100 ms) extend into the film a macroscopic distance, covering up to half the film area for a large pulse, before rapidly retreating to the edge. The complete process may leave the global film thickness unchanged, but can also initiate a thinning of one or more layers starting near the small heater. A second and related feature of this effect is the appearance of a spherical droplet created at or near the pulse heater immediately following the heat pulse. Both of these phenomena can be seen in Fig. 9. Although the exact details of this process are not fully determined, we propose a probable scenario. For an N -layer film, when $\Delta T_N [= T_C(N) - T]$ is small, the pulse amplitude $V_N(T)$ to produce a thinning is also correspondingly small. In this case we observe no meniscus involvement or droplet formation, and we assume the thinning occurs via a thermally nucleated dislocation loop. If we remain at the same film temperature, for the $(N-1)$ -layer film $\Delta T_{N-1} > \Delta T_N$ and accordingly $V_{N-1}(T) > V_N(T)$. Each successive thinning at temperature T requires a larger pulse voltage. For large voltages, the local thermal perturbation is very large and locally melts an internal region of material into the isotropic phase. If the melted interior material is surrounded by exterior Sm A layers, an interfacial energy cost will exist at the Sm A–isotropic interface. In order to reduce this energy, the material will tend to pull itself into a spherical droplet. Its radius (up to several hundred micrometers) is experimentally much larger (four or five orders of magnitude) than the thickness of the film. A droplet of this size contains more material than the entire film. It clearly contains not only material initially melted by

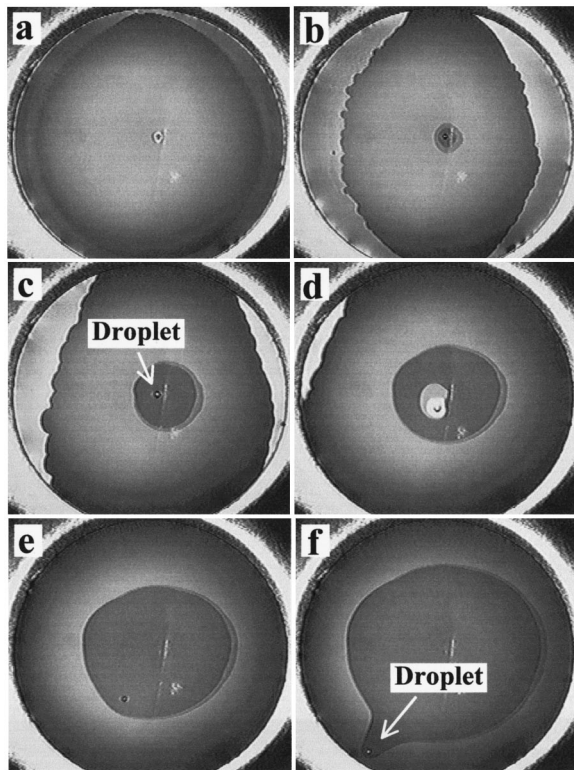


FIG. 9. Time evolution of a two-layer thinning with droplet formation and meniscus involvement. Immediately following the applied heat pulse, a droplet can be seen (a), (b). Material rushes in from the edge and two dislocation loops are formed (b) near the heater. In (c) and (d) the “meniscus” material quickly retreats and the dislocation loops grow rapidly, followed by slower growth in (e) and (f). The asymmetry of the retreating meniscus in (d) causes a shearing force that briefly flattens the droplet. The distortion of the thinning front caused by the droplet can be seen in (f).

the pulse, but also molecules from the reservoir. To form a 0.3-mm droplet in 0.1 s, a typical time frame, material must enter the film from the isotropic reservoir very rapidly (~ 50 cm/s) and increase in speed as it proceeds toward the droplet. During this time the film surrounding the droplet appears unchanged, indicating that the configuration of the material moving in from the edge is identical to the original film.

Apparently, if isotropic material enters the film to make up for material being pulled into the droplet, it rapidly arranges itself into smectic layers.

The meniscus involvement is now evident: the high speed of the moving layers drags thicker regions of material into the film. After the droplet is formed, the thick meniscus region quickly retreats (in a period of ~ 50 – 300 ms) and exerts a shear force on the remaining stable layers of the film. The droplet remains and is seen to be stable against this force, which should have the largest gradient and divergence at or near the location of the droplet formation. However, if the force is strong enough it can pull open a growing dislocation loop of one or more layers near the droplet location. In accordance with a nonsymmetric shearing force due to the observed irregularly shaped retreating meniscus, the shape of the dislocation loop is irregular at its formation. A second confirmation of this shearing force is that the irregular dislocation loop expands very rapidly initially, during the time the meniscus is retreating, before continuing at a slower, constant speed.

III. SUMMARY

In summary, we have thermally induced thinning transitions by nucleating dislocation loops in overheated Sm-A films at temperatures below $T_C(N)$ and measured their rate of expansion. The speeds obtained as a function of film thickness and temperature are qualitatively consistent with the proposed model of a thinning transition as the result of a nucleated dislocation loop. In addition, we have studied the interaction between two simultaneously growing dislocation loops, and find evidence for and the effects of an interlayer shear viscosity. Finally, we have given a qualitative explanation for the observed meniscus involvement and droplet formation observed under certain conditions.

ACKNOWLEDGMENTS

We are grateful to R. Holyst and P. Mach for their help and numerous discussions. We would like to thank Dr. M. D. Radcliffe (3M Corp. St. Paul, MN) for providing us with the sample. The experimental work reported here was supported in part by the National Science Foundation, Solid State Chemistry, Grant No. DMR 97-03898, and the Donors of the Petroleum Research Fund, administered by the American Chemical Society.

-
- [1] Ch. Bahr, *Int. J. Mod. Phys. B* **8**, 3051 (1994); T. Stoebe and C. C. Huang, *ibid.* **9**, 2285 (1995); Ch. Bahr, C. J. Booth, D. Fliegner, and J. W. Goodby, *Phys. Rev. Lett.* **77**, 1083 (1996).
- [2] J. Géminard, C. Laroche, and P. Oswald, *Phys. Rev. E* **58**, 5923 (1998).
- [3] S. Chandrasekhar, *Liquid Crystals*, 2nd ed. (Cambridge University Press, New York, 1992) pp. 80–84.
- [4] T. Stoebe, P. Mach, and C. C. Huang, *Phys. Rev. Lett.* **73**, 1384 (1994).
- [5] T. Stoebe, P. Mach, S. Grantz, and C. C. Huang, *Phys. Rev. E* **53**, 1662 (1996).
- [6] P. M. Johnson, P. Mach, E. D. Wedell, F. Lintgen, M. Neubert, and C. C. Huang, *Phys. Rev. E* **55**, 4386 (1997).
- [7] S. Pankratz, P. M. Johnson, H. T. Nguyen, and C. C. Huang, *Phys. Rev. E* **58**, R2721 (1998).
- [8] E. I. Demikhov, V. K. Dolganov, and K. P. Meletov, *Phys. Rev. E* **52**, R1285 (1995).
- [9] V. K. Dolganov, E. I. Demikhov, R. Fouret, and C. Gors, *Phys. Lett. A* **220**, 242 (1996).
- [10] A. J. Jin, M. Veum, T. Stoebe, C. F. Chou, J. T. Ho, S. W. Hui, V. Surendranath, and C. C. Huang, *Phys. Rev. E* **53**, 3639 (1996).
- [11] E. A. L. Mol, G. C. L. Wong, J. M. Petit, F. Rieutord, and W. H. de Jeu, *Physica B* **248**, 191 (1998).
- [12] P. Mach, P. M. Johnson, E. D. Wedell, F. Lintgen, and C. C. Huang, *Europhys. Lett.* **40**, 399 (1997).
- [13] L. V. Mirantsev, *Phys. Lett. A* **205**, 412 (1995).
- [14] Y. Martinez-Raton, A. M. Somoza, L. Mederos, and D. E.

- Sullivan, Phys. Rev. E **55**, 2030 (1997).
- [15] E. E. Gorodetsky, E. S. Pikina, and V. E. Podneks, Zh. Eksp. Teor. Fiz. **115**, 61 (1999) [JETP **88**, 35 (1999)].
- [16] J. Géminard, R. Holyst, and P. Oswald, Phys. Rev. Lett. **78**, 1924 (1997).
- [17] S. Pankratz, P. M. Johnson, R. Holyst, and C. C. Huang, Phys. Rev. E **60**, R2456 (1999).
- [18] Figure 3 shows that the thinning velocity varies strongly with temperature. Constant thinning speed, similar to the one shown in Fig. 2, has been obtained from all our data of local heater-induced thinning transitions. This gives us a clear indication that film temperature is reasonably uniform throughout the thinning process.
- [19] L. Lejcek and P. Oswald, J. Phys. II **1**, 931 (1991).
- [20] P. G. de Gennes, Langmuir **6**, 1448 (1990).